

Multi-virion infectious units arise from free viral particles in an enveloped virus

Supplementary Information

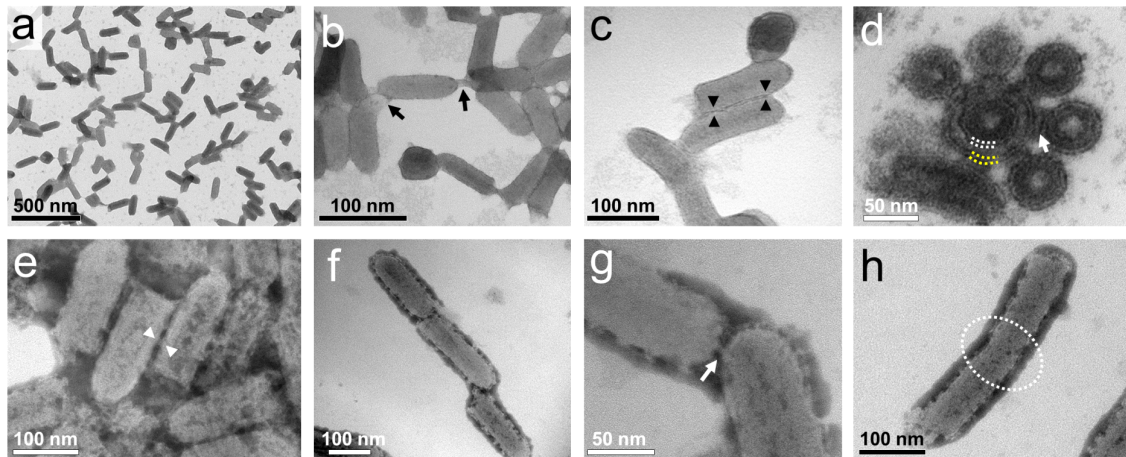
José M. Cuevas, María Durán-Moreno, and Rafael Sanjuán

Supplementary Table 1. Flow cytometry data used in co-fluorescence tests (Excel format).

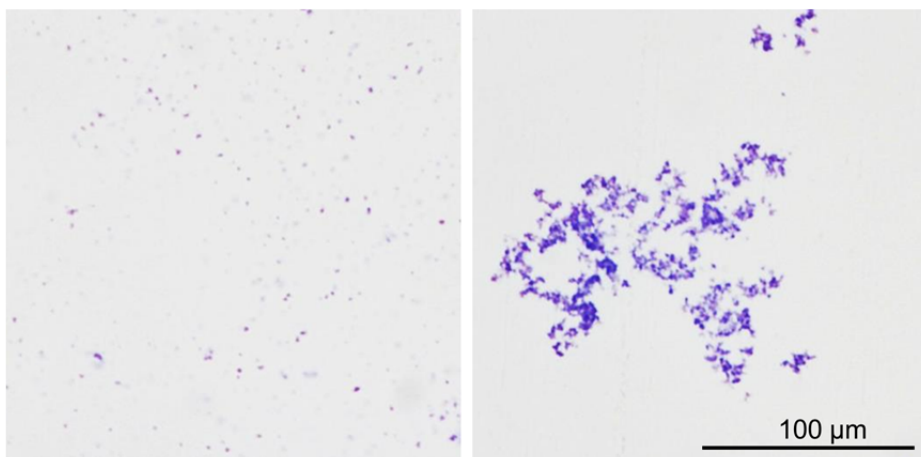
Supplementary Table 2. Flow cytometry cell counts for trypsin-treated viruses^a.

Experimental conditions			Observed cell counts			
Initial titer	Incubation conditions	Time post inoculation	Uninfected	GFP only	Cherry only	GFP+Cherry
1.50E+11	Untreated	4 h	91492	25	621	8
1.50E+11	Untreated	4 h	91584	32	947	5
1.50E+11	37°C, 2 h	4 h	90148	86	866	554
1.50E+11	37°C, 2 h	4 h	87764	57	897	483
1.50E+11	Untreated	6 h	82026	26	3751	13
1.50E+11	Untreated	6 h	80233	19	4555	16
1.50E+11	37°C, 2 h	6 h	76581	1683	4702	4866
1.50E+11	37°C, 2 h	6 h	71734	2354	4785	6488

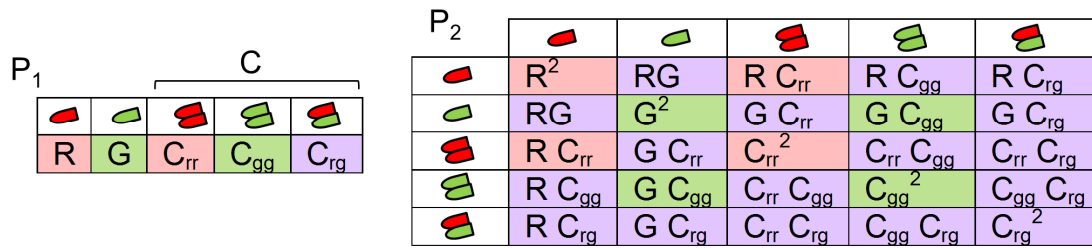
^aData from **Fig. 3**.



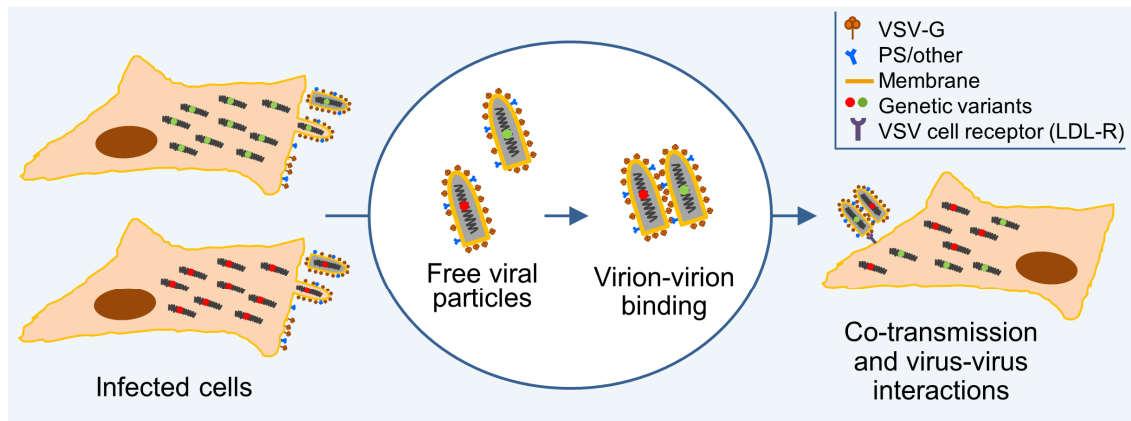
Supplementary Figure 1. Electron micrographs of purified VSV virions. **a.** Overview of a virion suspension positively stained with uranyl acetate. **b.** Magnified view of a similar preparation, showing virion-virion contacts and partial deformation of a virion (arrows). **c.** Similar preparation showing lateral contacts alongside two virions. **d.** Ultrathin section of agar-encased VSV virions showing a unique structure in cross section, in which a central virion is surrounded by an extra lipid bilayer (yellow dotted lines) outside the normal envelope (white dotted lines), and five virions are longitudinally attached to the outermost bilayer of the central virion (arrow). **e.** Virion suspension negatively stained with phosphotungstic acid showing lateral contacts between virions. One such contact is indicated. **f.** Similar preparation showing lateral contacts between virions. One such contact is indicated. **g.** Detail of one of these base-top contacts. **h.** Rare instance of apparently fused virions.



Supplementary Figure 2. Light microscopy of VSV virion aggregates. Virions were fixed, stained with toluidine blue, and imaged at 100-fold magnification in a conventional light microscope. Left: untreated. Right: incubated at 37°C overnight.



Supplementary Figure 3. Probabilistic model for inferring the fraction of inoculum virions bound to other virions. The model considers five possible types of PFUs: the two types of single virions (red and green with frequencies R and G, respectively) and the three possible dual complexes resulting from virion-virion binding (red/red, C_{rr}; green/green, C_{gg}; red/green, C_{rg}). This is a simplification, since experimental data suggest that larger aggregates also formed. The total frequency of dual complexes in the model is thus $C = C_{rr} + C_{gg} + C_{rg}$, and, since higher-order aggregates were not considered, $R + G + C = 1$. The four observable variables are the proportion of non-infected (P_0), mCherry-only positive (P_R), GFP-only positive (P_G), and mCherry/GFP doubly fluorescent (P_{RG}) cells obtained from flow cytometry counts. We inferred the MOI as $\exp(-P_0)$, and the fraction of cells receiving one (P_1) and with two (P_2) PFUs was estimated using a Poisson distribution with mean equal to this MOI. Since the MOI was low, $P_0 + P_1 + P_2$ was > 0.9995 in all cases and we hence ignored the probability of three or more PFUs per cell. As shown in the figure, the observables P_R , P_G , and P_{RG} (red, green and purple shadowing, respectively) depend on model parameters as follows: $P_R = P_1(R + C_{rr}) + P_2(R^2 + 2RC_{rr} + C_{rr}^2)$, $P_G = P_1(G + C_{gg}) + P_2(G^2 + 2GC_{gg} + C_{gg}^2)$, and $P_{RG} = P_1C_{rg} + P_2(1 - R^2 - 2RC_{rr} - C_{rr}^2 - G^2 - 2GC_{gg} - C_{gg}^2)$. Furthermore, in a well-mixed virion suspension the frequencies of each type of dual complex should obey the following proportions: $C_{rr}/C = R^2/(R + G)^2$, $C_{gg}/C = G^2/(R + G)^2$, and $C_{rg}/C = 2RG/(R + G)^2$. Hence, parameters C, C_{rr}, C_{gg}, and C_{rg} can all be expressed in terms of R and G such that, in the model, P_R , P_G , and P_{RG} depend solely on R and G. A numerical solution was obtained by finding the values of R and G that minimized the sum of squared residuals between predicted and observed cell counts, and the proportion of dual complexes was then obtained as $C = 1 - R - G$. The estimated proportion of virions in dual complexes, $2C/(2C + R + G)$, is reported in the text and figures.



Supplementary Figure 4. Schematic representation of virion-virion binding and co-transmission. Infected cells release enveloped virions by budding. These virions contain cell-derived components in their envelopes, including PS. In the extracellular milieu, interactions between the virus-encoded surface protein G and PS/other components lead to the establishment of virion-virion complexes and to subsequent co-transmission of the attached particles to new cells. Entry of one of the virions is sufficient for dragging other, attached virions, into the cell. Attached particles can originate from different cells, allowing different genetic variants of the virus to be combined into multi-virion infectious units. These variants can then establish functional interactions.